

DEVELOPMENT OF A FUEL THERMAL DIFFUSIVITY MEASUREMENT TECHNIQUE USING PULSED ELECTRON BEAMS

M.S. DE JONG, F.P. ADAMS, R.M. HUTCHEON, P.G. LUCUTA AND R.A. VERRALL

Chalk River Laboratories, Chalk River, Ontario, Canada K0J 1J0

Abstract

A new technique is being developed for measuring the thermal diffusivity of materials using a 11.4 MeV electron beam. A short, high-current pulse (≈ 0.1 second) of high-energy electrons penetrates axially into one end of a cylindrical sample whose length is a few times the electron range. Thermocouples or remote heat-sensing devices measure the resultant time-dependent temperature distribution on the other end of the sample. A comparison with both reference standards and theoretical predictions allows one to determine the thermal diffusivity. The errors are the result of uncertainties in (1) the pulse timing (which is small), (2) the electron penetration distribution, and (3) the rate of heat-loss to the surroundings. Initial proof-of-principle measurements on a fresh UO_2 CANDU reactor fuel pellet demonstrated accuracy and reproducibility with a statistical error of $\leq \pm 6\%$. An added benefit of the technique is that it simultaneously measures the fractional change in the specific heat with temperature.

1. INTRODUCTION

This paper describes a new technique for measuring the axial thermal diffusivity of a reactor fuel pellet. The thermal diffusivity, $\alpha(\text{m}^2 \cdot \text{s}^{-1})$, is a measure of the rate of propagation of a heat pulse through a material and, together with the specific heat, $C_p(\text{kJ} \cdot \text{K}^{-1} \cdot \text{kg}^{-1})$, determines both the transient and steady-state fuel operating temperatures. The thermal conductivity, $\lambda(\text{kW} \cdot \text{K}^{-1} \cdot \text{m}^{-1})$, is obtained from the product of the thermal diffusivity, the specific heat, and the density, $\rho(\text{kg} \cdot \text{m}^{-3})$:

$$\lambda(T) = \alpha(T) \cdot C_p(T) \cdot \rho(T). \quad (1)$$

The present technique is conceptually similar to the laser-flash diffusivity technique,⁽¹⁾ and is based on the rapid, pulsed heating of one end of a cylindrical sample - using a high-power, 11.4 MeV electron beam - and measuring the temperature response of the backface of the fuel sample. The sample is mounted with only a few sharp contact points to reduce heat-loss to the surroundings. Some advantages of the present technique over laser flash are: a larger amount of energy is available to be absorbed in the sample permitting the use of larger or thicker samples, the absorbed energy is distributed over a significant thickness of the material resulting in small instantaneous temperature rises over small portions of the sample, and the absorbed energy is independent of sample reflectivity or temperature.

The theory for the time-dependent evolution of the spatial distribution of temperature in a cylindrical sample is well established, and the specific approximations suitable to the present experiment

will be mentioned. The initial distribution of temperature (i.e. the initial conditions for the time evolving problem) are determined using a well-known and validated electron/photon Monte Carlo transport code, ITS-CYLTRAN-p.⁽²⁾ The thermal response of the backside of the pellet was measured with thermocouples, and the theory was suitably modified to take into account thermocouple response times. The theoretical response function had three free parameters with which to fit the data: the diffusivity, the average temperature rise caused by the beam pulse (proportional to C_p) and the rate of heat loss to the surroundings (a very small correction at present temperatures).

The axial thermal diffusivity of an 8.02 mm long, 12.5 mm diameter section of an unirradiated Bruce UO₂ fuel pellet was measured to test the technique. The theoretical response fitted the data very well, yielding small statistical errors. The relative specific heat as a function of temperature seemed also to be well determined. It appears that the systematic errors associated with the technique will determine the ultimate uncertainty, and can only be evaluated through more measurements using different geometries and materials.

2. DESCRIPTION OF THE MEASUREMENT SYSTEM

The measurement system consists of an electron accelerator delivering pulses of electrons into a vacuum chamber (Fig. 1), where a cylindrical specimen is held thermally isolated from its surroundings. A small radiant heater maintains the sample and its surroundings at the required ambient temperature. Thermocouples pressed against the sample backface measure the temperature as a function of time. The digitally-stored data is later fitted by the theory to extract the thermal diffusivity and the relative specific heat.

a) Pulsed Electron Beam

The electron beam is generated by the Pulsed, High-Energy Electron Linear Accelerator (PHELA) at AECL's Chalk River Laboratories. The accelerator is a 3 GHz on-axis-coupled-cavity linac, driven by a klystron rf (radio frequency) power generator. The klystron generates 5.9 micro-second long rf power pulses at a maximum rate of 250 pulses per second. The output electron beam current during the 5.9 microsecond pulse has a mean value of 200 milliamperes at a mean output energy of 11.4 MeV. The latter was determined by the aluminum-wedge technique.¹⁽³⁾ The beam at the accelerator exit has very low divergence and is ≈ 5 millimetres diameter. For the present measurements, the accelerator was turned on for 25 pulses (at a rate of 250 pulses per second), producing a 100 millisecond long "macropulse" with 305 microamperes mean current during the pulse. Thin, air-cooled foils of titanium alloy (Ti6Al4V, ≈ 150 microns thick) are used as vacuum windows to separate the accelerator structure vacuum ($\leq 10^{-7}$ Torr) from the sample chamber atmosphere.

It should be noted that a linac is a very simple device with very stable output current and energy. The energy is governed by rf power levels which are regulated to $\leq \pm 2\%$, and the beam current is governed by gun spatial geometry and dc bias voltage - both very stable. Thus, although the absolute value of the beam current and energy may have some systematic uncertainty, the relative values over many hours and days are very reproducible. This means that the beam deposits a very reproducible amount of energy in the sample regardless of the ambient temperature of the sample, and thus the relative temperature increment at each temperature is directly proportional to the value of the specific heat at that temperature.

b) Target Chamber and Sample Mount

The physical layout of the vacuum windows, the target chamber and the sample and sample mount is shown in Fig. 1. The distance between the dual, thin-window foils and the sample was set so that multiple-scattering in the foils would introduce sufficient divergence in the beam to achieve less than 10% variation in the intensity of illumination of the sample front face, while maintaining sufficient current per unit area to produce an easily-measurable temperature pulse. A collimator was placed upstream of the sample to shield the sample mount and target chamber from the scattered electron beam. Approximately 10% of the beam actually intercepted the sample. The sample was suspended in a simple cage of stainless steel wire which was in good contact with the 12.7 mm ID stainless steel tube. The larger chamber behind the sample mounting tube was used for the thermocouple mounting jig and for easy mounting of pumping and gas-handling ports. The present measurements were performed with ≈ 1 atmosphere argon backfilled into the system.

c) Thermocouple Temperature Measurement and Data Logging Systems

A schematic view of the mounting technique of the thermocouples is shown in Fig. 1. The temperature rise on the back face of the sample was expected to be $\approx 10^\circ\text{C}$. Because high temperatures were not required for initial demonstration experiments, type J, 0.25 mm diameter, sheathed thermocouples (maximum temperature of 500°C) were chosen because of their high sensitivity. The sheathed type of thermocouple was used to reduce electrical noise pickup from the electron beam and the klystron drive pulse. A small-diameter (0.25 mm) thermocouple was chosen to minimize the inherent response time to a temperature pulse. It was necessary to independently spring-load the thermocouples against the pellet backface - anything less than positive loading force produced a clear increase in "thermal resistance" between the sample and a thermocouple.

The actual response time of the thermocouples was determined by measurements on copper samples having a known high value of thermal diffusivity and thus showing a known, fast response to the beam pulse. The fitted data and the extracted value of the "effective RC equivalent circuit" response time are shown in Fig. 2.

3. THEORETICAL DESCRIPTION OF THE SAMPLE THERMAL RESPONSE

Fitting the measured data requires a solution of the time-dependent thermal response of the sample to an effectively instantaneous deposition of distributed heat in the bulk of the sample. The response of the sample at the location of the thermocouple (the backface in this case) must then be folded with the thermocouple response function to achieve a representation of the data. In the present case, the beam and the sample can be represented in cylindrical coordinates with no azimuthal dependence - i.e. azimuthal symmetry is assumed for all properties. Under these conditions, the time-dependent thermal diffusion equation for the situation where no heat is generated inside the sample is given by

$$\frac{1}{r} \frac{\partial}{\partial r} \left[r \frac{\partial T}{\partial r} \right] + \frac{\partial^2 T}{\partial z^2} - \frac{1}{\alpha} \frac{\partial T}{\partial t} = 0, \quad (2)$$

where the homogeneous solutions have the form

$$T(r, z, t) = U(r)V(z)W(t) \quad (3)$$

and the solutions are obtained by the separation of variable technique:

$$T_{\ell,n}(r, z, t) = J_0(\nu_\ell r) \cdot \cos(n\pi z/L) \cdot e^{-\alpha[\nu_\ell^2 + (n\pi/L)^2]t}, \quad (4)$$

where $n = 0, 1, 2, \dots, L$ is the sample length, and the values of ν_ℓ ($\ell = 1, 2, 3, \dots$) are determined by the radial boundary conditions. Assuming only a small radial heat loss and a nearly-uniform radial electron beam density, the time response of the pellet can be described as a Fourier sum over the axial modes while retaining only the single lowest order radial term in the expansion ($\ell = 1$):

$$\Delta T(z, t) = \Delta T_0 e^{-\alpha \nu_1^2 t} \left(\sum_{n=0,1,2,\dots} Fc_n \cdot \cos(n\pi/L) \cdot e^{-\alpha(n\pi/L)^2 t} \right), \quad (5)$$

where Fc_n are Fourier coefficients, determined by the fit to the initial, instantaneous, axial temperature distribution produced in the pellet by the electron pulse at $t = 0$, and the value of ν_1 is determined by the fit to the slow decrease of the pellet temperature after the fast thermal transient.

The initial, mean axial, temperature distribution was obtained using the ITS - Monte Carlo code, which simulates the energy transport and deposition in materials produced by an incident projectile. It is a full 3-dimensional code, so the experimental arrangement of dual thin foils, drift to the pellet, stainless steel vacuum chamber and sample were all modeled. The mean axial energy deposition was obtained by conceptually slicing the sample into 0.5 mm thick discs and having the code calculate the energy deposited in each disc (Fig. 3). The resultant axial distribution was used to calculate the Fourier coefficients in eq. (5) up to the 16th order ($n=16$), which produced good theoretical fits to the initial temperature distribution as typified by the curve shown in Fig. 3.

The theoretical response of the sample backface for a given ambient temperature, T_a , was obtained by evaluating eq. (5) at $z = L$:

$$\Delta T(L, t) = \Delta T_a \left[\sum_{n=0,1,\dots} (-1)^n Fc_n e^{-\alpha[\nu_1^2 + (n\pi/L)^2]t} \right], \quad (6)$$

where ΔT_a , α and ν_1 are functions of the ambient temperature, and in which the Fourier coefficients are normalized so that $Fc_0 = 1$. This results in ΔT_a being inversely proportional to the specific heat if the energy delivered to the sample is maintained constant:

$$C_p(T_a) = \frac{\Delta E_{\text{beam}}(kJ)}{\Delta T_a \cdot M_s(kg)}, \quad (7)$$

where M_s is the sample mass, and ΔE is the energy deposited by the beam in the sample. The final consideration in modeling the complete system response is to include the correction for the thermocouple response. Considering the thermocouple response to be simulated by a series RC network (response time τ_{tc}), in series with the backface response of the pellet, the following modification of eq. (6) gives the equation for the measured thermocouple output:

$$\Delta T_{tc}(t) = \Delta T_a \left[\sum_{n=0,1,2,\dots} \frac{(-1)^n Fc_n}{(1 - \tau_{tc} \cdot \alpha \cdot [\nu_1^2 + K_n^2])} (e^{-\alpha[\nu_1^2 + K_n^2]t} - e^{-t/\tau_{tc}}) \right], \quad (8)$$

where

$$K_n = (n\pi/L).$$

Fitting eq. (8) to the measured backface response of an 11 mm long, 12.5 mm diameter copper pellet (thermal diffusivity, $\alpha = 113 \times 10^{-6} m^2 s^{-1}$), using the same thermocouples and thermocouple mounting system, resulted in a value of $\tau_{tc} = 0.256$ seconds (Fig. 2). A large variation of this value

has very little influence on the measured diffusivity value, when the sample response time is 2.5 seconds or more.

4. DETERMINATION OF THE THERMAL DIFFUSIVITY AND SPECIFIC HEAT

A typical set of measurements over a broad temperature range is accomplished in one day. The sample is mounted in its cage and the thermocouple mounting fixture is checked for positive loading force and then fixed in place. The chamber is sealed up, evacuated and back-filled a few times, and then filled to the required pressure. The ambient heater is used to bring the sample to the required temperature, as measured by the backface temperature. Then, upon operator request, the control/data logging system starts recording the backface thermocouple temperature at a rate of 250 Hz (i.e. every 4 milliseconds). Two seconds after initiating the data logging, the control system turns on the accelerator for 25 machine pulses at the same 250 Hz rate, synchronized to the same pulse generator. The result is a 100 millisecond macropulse, synchronized to the data logging timing. The system continues logging thermocouple data at the 250 Hz rate for up to 60 seconds. After this sequence, the ambient temperature is set to the next desired value and the sequence repeated.

Data reduction and fitting to the theory is all done off-line. The first step is to reduce the noise on the digitized thermocouple response by averaging 25 consecutive thermocouple measurements and associating this value with the mean time of the 25 measurements. A typical measurement of the thermocouple response, averaged in this way, is shown in Fig. 4, and typically has a 0.03°C r.m.s. temperature variation in the flat region before the pulse. This data reduction results in 10 temperature points per second with a spacing equal to the beam pulse width.

In the general case, the data would be fitted using eq. (8), with the value of the thermocouple response time pre-determined by measurements on a copper pellet. In the present case, the pellet was well isolated from its surroundings and the heat loss factor, ν_1 , was very small (Fig. 4). Thus the values presented here result from a three parameter fit, in which α , ΔT_a and ν_1 were varied to produce a minimum r.m.s. temperature variation (typically $\leq 0.06^{\circ}\text{C}$) between the data and eq. (8), starting the fit 0.3 seconds after the beam pulse. Each measurement was performed six times at each temperature. The six values of α and ΔT_a determined for each temperature were averaged, and the average values are shown in Fig. 5. The error shown is the rms spread of each six values.

The relative values of the specific heat were determined using eq. (7) and assuming the beam pulse delivered a constant energy to the sample at all temperatures. The six values determined at each temperature were averaged, and the curve normalized at 200°C to those of Lucuta.⁽⁴⁾ The errors represent the rms variation of each set of six values.

5. CONCLUSIONS

The results of the first set of axial thermal diffusivity measurements on a UO_2 pellet suggest that the electron beam pulse method will be a viable technique. The accuracy achievable with the technique appears to be better than $\pm 5\%$, and will be limited by systematic errors since the statistical error can be made quite small. Clearly, many more measurements with different geometries of sample, sample holder and thermocouple mounting are required to establish systematic error limits. The influence of the uncertainty in the initial electron energy distribution can be determined using the ITS Monte Carlo code. Work is underway to build the required transfer flasks and target chambers to allow measurements on irradiated fuel.

The technique also appears capable of simultaneously measuring the relative specific heat of the material, although this does rely completely on the linearity of the temperature pulse measurement technique. This will require careful control and checking of systematic errors, such as, in the present case, the influence of temperature on the effective thermal contact resistance between the thermocouple and the pellet.

Acknowledgements

We wish to thank the Accelerator Physics Branch electron beam development team, whose interest and dedication made the evolution of a new system seem easy.

References

1. H. BRÄUER, L. DUSZA, B. SCHULTZ, "New Laser Flash Equipment LFA 427", *Interceram* 41 (1992) 7/8, 489-492.
2. J.A. HALBLEIB, R.P. KENSEK, T.A. MEHLHORN, G.D. VALDEZ, S.M. SELTZER, M.J. BERGER, "ITS Versin 3.0: The Integrated TIGER Series of Coupled Electron/Photon Monte Carlo Transport Codes", *SAND91-1634-UC-405*.
3. "Standard Practice for Dosimetry in an Electron Beam Facility for Radiation Processing at Energies Between 300 keV and 25 MeV". American Society for Testing & Materials, 1916 Race St. Philadelphia, Pa 19102; ASTM Designation E 1649-94.
4. P.G. LUCUTA, H.J. MATZKE, R.A. VERRALL and H.A. TASMAN, "Thermal Conductivity of SIMFUEL", *J. Nuclear Materials* 188 (1992) 198-204.

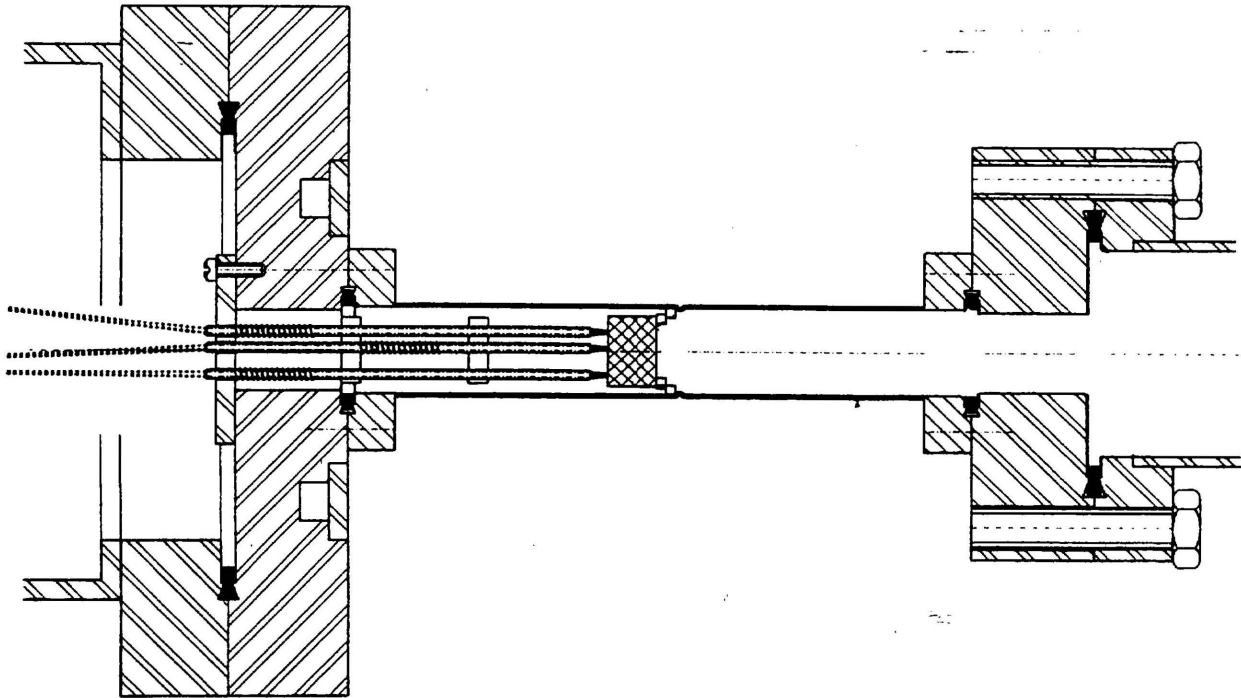


Fig. 1. A section of the target chamber, showing the pellet mounting technique, the spring-loaded thermocouples. The electron beam enters from the right.

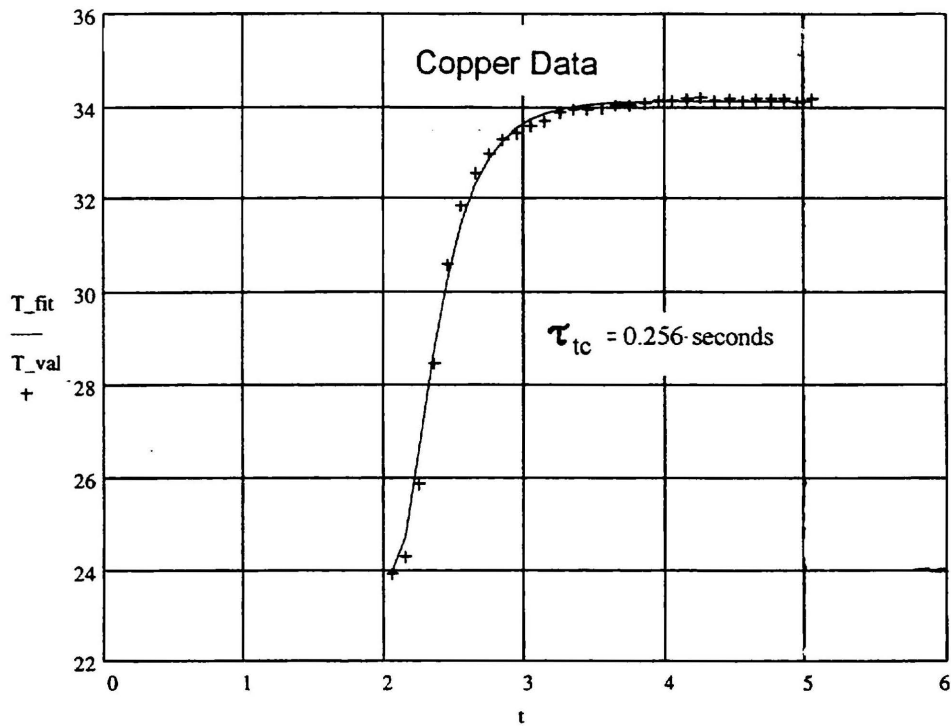


Fig. 2. A measured temperature-versus-time response curve for a long copper pellet, used to determine the thermocouple response time.

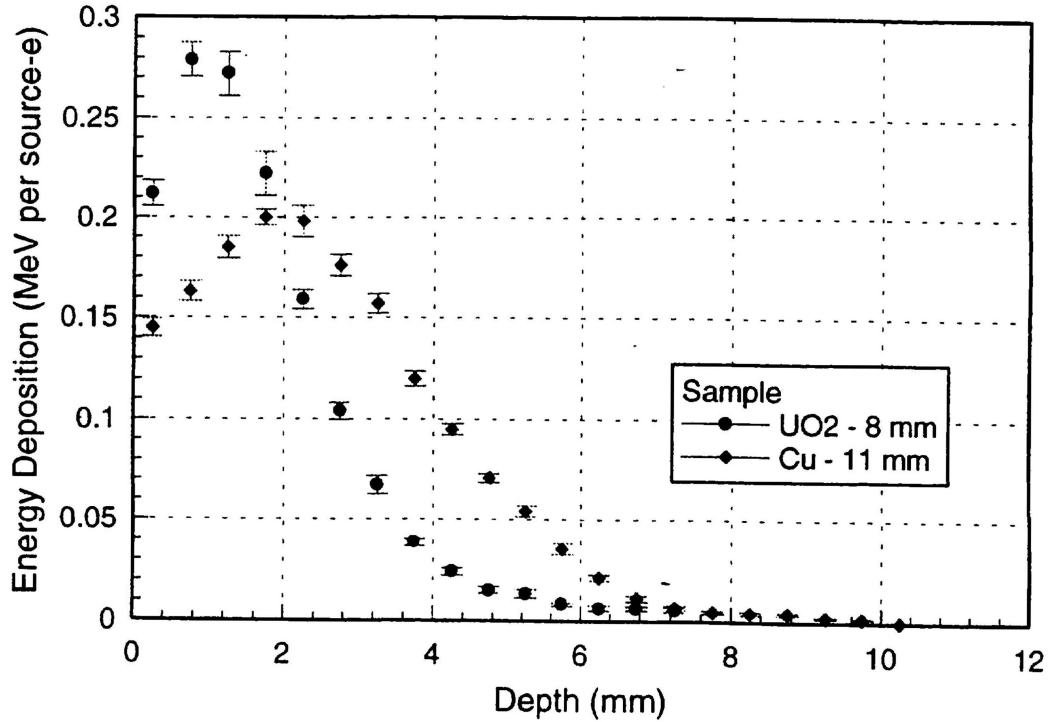


Fig. 3. The initial axial distribution of energy deposition in the UO_2 pellet and the 11 mm long copper calibration pellet calculated using the ITS Monte Carlo code. These distributions give the initial conditions for the time-dependent theory.

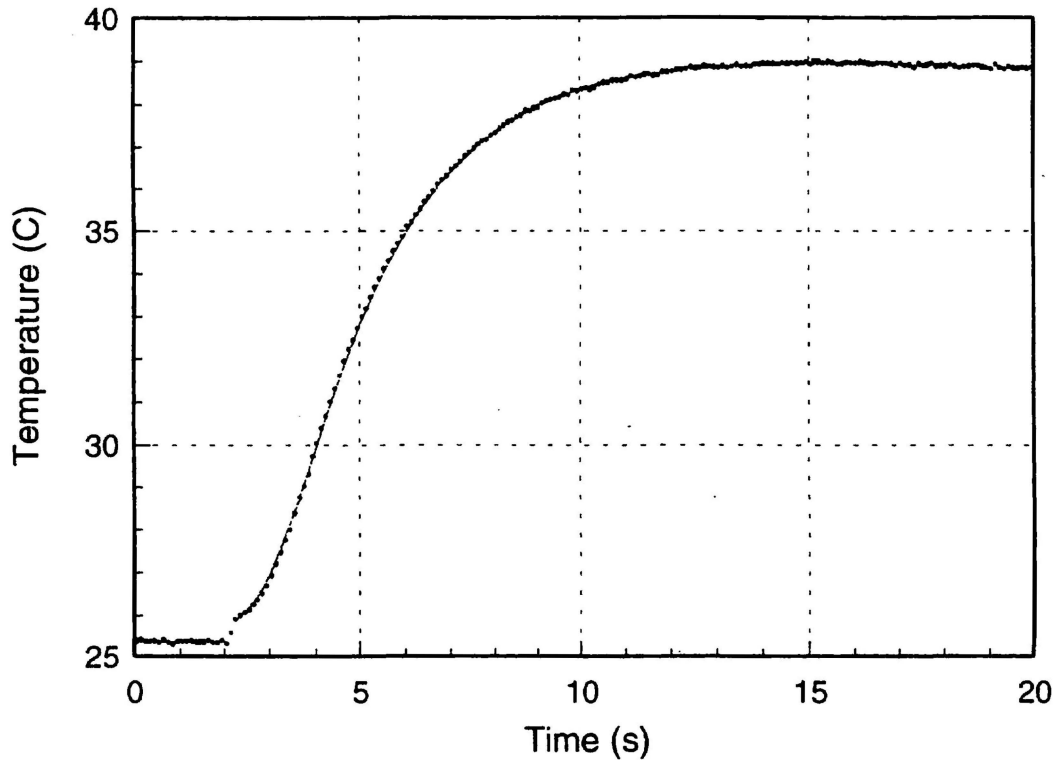


Fig. 4. A back-face temperature versus time response curve for an 8.02 mm long, high density UO_2 pellet, heated by a 100 ms long, 11.4 MeV electron pulse, incident on the front face. The line is a two parameter fit ($\nu_1 = 0$) using eq. 8, with $\alpha = 2.64 \times 10^{-6} \text{ m}^2 \cdot \text{s}^{-1}$ and $\Delta T_a = 13.6^\circ\text{C}$.

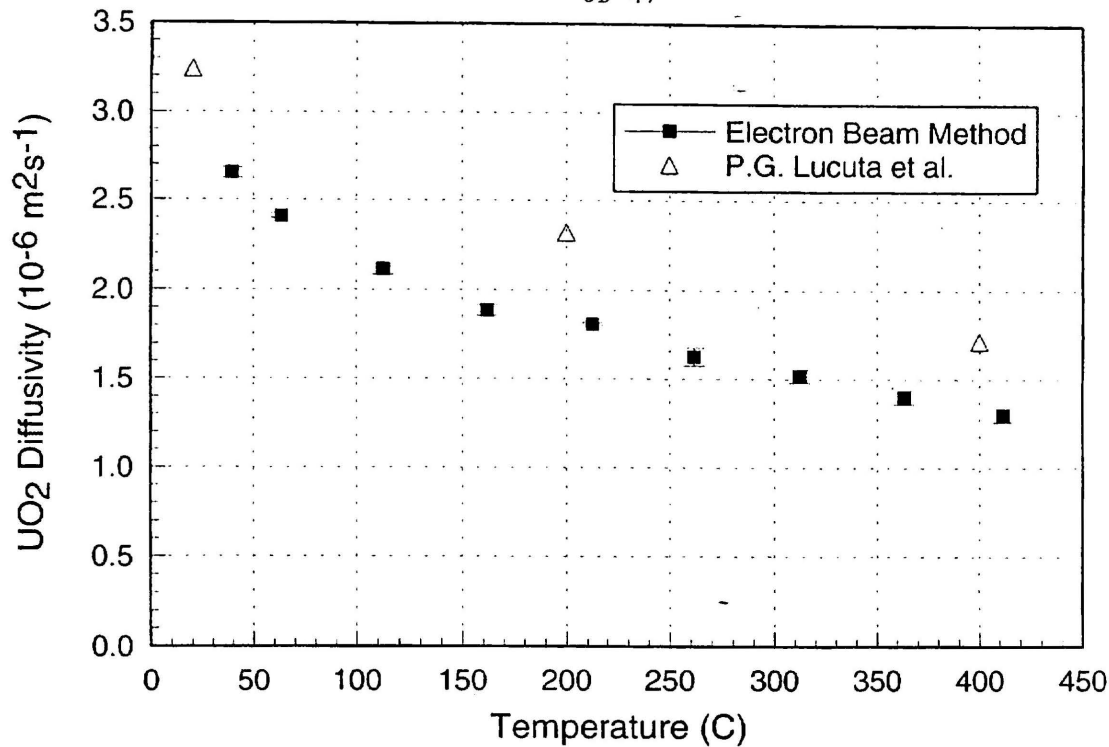


Fig. 5. The measured thermal diffusivity, using the electron beam technique, of an 8.02 mm long section of a Bruce fuel pellet (density 10.73 ± 0.02 gm/cc) in an argon atmosphere. The triangles are measurements on UO₂ of density 10.785 gm/cc, using the laser flash technique (Ref. 3).

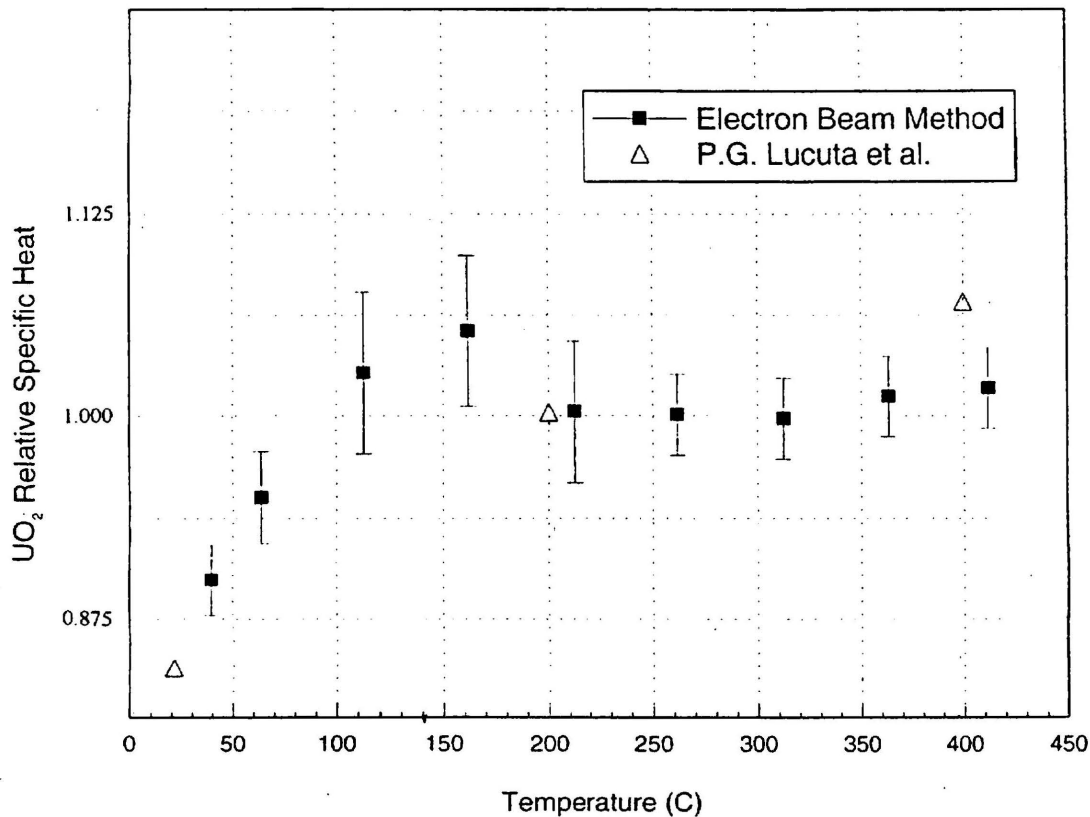


Fig. 6. The measured *relative* specific heat using the electron beam technique. The values are normalized to those of Ref. 3 at 200°C.